Transactions on Modelling and Simulation vol 3, © 1993 WIT Press, www.witpress.com, ISSN 1743-355X

A boundary element analysis of magnetic fields near surfaces

H. Igarashi, T. Honma

Department of Electrical Engineering, Faculty of Engineering, Hokkaido University, Kita 13, Nishi 8, Kita-ku, Sapporo, 060 Japan

ABSTRACT

This paper describes a boundary element method for accurate computation of magnetic fields near surfaces of magnetic materials. The present method, which includes two different approaches, is based on the regularization of the quasi singularity in the kernel. The numerical results show that the present method gives accurate magnetic fields near the surface of a magnetic material of a rectangular cross section.

INTRODUCTION

Design of equipment employing magnetic materials such as magnetic heads and magnets requires highly accurate evaluation of magnetic fields especially near an iron core and in an air gap. The boundary element method (BEM) seems suitable for the computation of the magnetic field of magnetic equipment because they often have considerably fine air gaps compared to size of the iron core, and moreover the magnetic field in infinite regions around magnetic materials must be effectively calculated.

However, it is known that the conventional BEM based on the Gaussian quadrature can not give an accurate potential and its gradient near boundaries and material surfaces because of the quasi singularity in the kernel.

Recently, the authors have developed the computational methods [1] which give accurate values of the potential and its gradient at arbitrary points in the domain.

In this paper, after the above mentioned methods are outlined, they are applied to an analysis of the magnetic field around a two dimensional magnetic material of a rectangular cross section.

FORMULATION FOR STATIC MAGNETIC FIELD

We here outline a boundary element formulation with the reduced scalar potential for static magnetic fields.

The reduced scalar potential

Let us consider a static magnetic field induced by an external current, as shown in Fig. 1. The governing equations of static magnetic fields are

$$\nabla \times \mathbf{B} = \mu_0 \mathbf{J}, \tag{1}$$

$$\nabla \cdot \mathbf{B} = 0, \tag{2}$$

where $\mathbf{B}$ is the magnetic flux density, μ_0 the permeability of vacuum and $\mathbf{J}$ is the current density. The magnetic field $\mathbf{H}$, which is related to the magnetic flux density by $\mathbf{B}=\mu_0\mu\mathbf{H}$, where μ is the relative permeability of material, can be divided into the solenoidal and irrotational components. The solenoidal component $\mathbf{H}_e$ is produced by the external current $\mathbf{J}_e$

$$\nabla \times \mathbf{H}_e = \mathbf{J}_e, \tag{3}$$

i.e.,

$$\mathbf{H}_e = \frac{1}{4\pi}\int_{\Omega_s} \frac{\mathbf{J}_e(\mathbf{r}') \times (\mathbf{r}-\mathbf{r}')}{|\mathbf{r}-\mathbf{r}'|^3}\, d\Omega'. \tag{4}$$

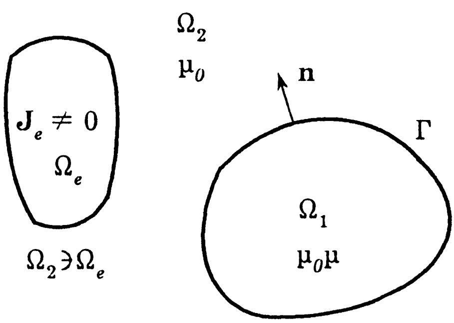

Fig. 1 Magnetic material immersed in a magnetic field. The material and vacuum regions are denoted by Ω_1 and Ω_2, respectively.

The irrotational component $\mathbf{H}_m$ produced by magnetization of a magnetic material is written in terms of the reduced scalar potential ϕ as follows :

$$\mathbf{H}_m = -\nabla\phi . \tag{5}$$

Substituting (5) into (2), we obtain for regions Ω_1 and Ω_2

$$\nabla^2\phi = 0 , \tag{6}$$

provided that the magnetic material has a linear permeability μ.

Continuity of the tangential component of $\mathbf{H}$ and the normal component of $\mathbf{B}$ on the surface Γ requires the boundary conditions

$$\phi_1 = \phi_2 , \quad \mu\left(\mathbf{n}\cdot\mathbf{H}_e - \frac{\partial\phi_1}{\partial n}\right) = \left(\mathbf{n}\cdot\mathbf{H}_e - \frac{\partial\phi_2}{\partial n}\right), \tag{7}$$

where the suffixes 1, 2 represent the quantities in the material and vacuum regions, respectively.

The solution of (6) under the boundary condition (7) gives the magnetic field $\mathbf{H}$ for a given external current.

<u>Boundary Element Formulation</u>

Equation (6) with the boundary condition (7) can be easily solved by BEM as described below. The correspondence $(u, v) \rightarrow (\phi, G)$ in Green's theorem

$$\int_\Omega (u\nabla^2 v - v\nabla^2 u)\, d\Omega = \int_\Gamma \left(u\frac{\partial v}{\partial n} - v\frac{\partial u}{\partial n}\right) d\Gamma , \tag{8}$$

leads to the integral equation for Ω_1

$$C_1(\mathbf{r})\,\phi_1(\mathbf{r}) = \int_\Gamma \left[G(\mathbf{r}';\mathbf{r})\frac{\partial\phi_1(\mathbf{r}')}{\partial n'} - \phi_1(\mathbf{r}')\frac{\partial G(\mathbf{r}';\mathbf{r})}{\partial n'} \right] d\Gamma' , \tag{9}$$

where C_1 is a constant dependent on geometry of Γ and G is the fundamental solution of the Laplace equation. Similarly, the integral equation for Ω_2 takes the form

$$C_2(\mathbf{r})\,\phi_2(\mathbf{r}) = -\int_\Gamma \left[G(\mathbf{r}';\mathbf{r})\frac{\partial\phi_2(\mathbf{r}')}{\partial n'} - \phi_2(\mathbf{r}')\frac{\partial G(\mathbf{r}';\mathbf{r})}{\partial n'} \right] d\Gamma' . \tag{10}$$

Note here that $\mathbf{n}$ is defined as the normal unit vector in the *outward* direction. Imposing the boundary conditions (7) to (9) and (10), and using the relation $C_1 + C_2 = 0$, we obtain the simultaneous equation

$$C_1(\mathbf{r})\,\phi_2(\mathbf{r}) = \int_\Gamma \left[G(\mathbf{r}';\mathbf{r}) \left\{ \left(1-\frac{1}{\mu}\right)\mathbf{n}\cdot\mathbf{H}_e + \frac{1}{\mu}\frac{\partial\phi_2(\mathbf{r}')}{\partial n} \right\} - \phi_2(\mathbf{r}')\,\frac{\partial G(\mathbf{r}';\mathbf{r})}{\partial n'} \right] d\Gamma',$$

$$[1-C_1(\mathbf{r})]\,\phi_2(\mathbf{r}) = -\int_\Gamma \left[G(\mathbf{r}';\mathbf{r})\,\frac{\partial\phi_2(\mathbf{r}')}{\partial n'} - \phi_2(\mathbf{r}')\,\frac{\partial G(\mathbf{r}';\mathbf{r})}{\partial n'} \right] d\Gamma'. \tag{11}$$

The usual boundary element discretization of (11) produces the linear matrix equation for the unknown variables $[\phi_2]_i$ and $[\partial\phi_2/\partial n]_i$, which can be readily solved by an appropriate numerical technique.

REGULARIZED FORMULAE

We here describe two regularized formulae for the gradient $\nabla\phi$ in the outer region Ω_2. The approaches described below can be easily modified to those for closed boundary problems [1].

In a usual boundary element analysis, after finding the boundary potentials and fluxes, the field gradient in Ω_2 is computed from

$$\nabla_{\mathbf{r}}\phi_2(\mathbf{r}) = -\int_\Gamma \left[\frac{\partial\phi_2(\mathbf{r}')}{\partial n'}\nabla_{\mathbf{r}} G(\mathbf{r}';\mathbf{r}) - \phi_2(\mathbf{r}')\,\nabla_{\mathbf{r}}\frac{\partial G(\mathbf{r}';\mathbf{r})}{\partial n'} \right] d\Gamma' \tag{12}$$

to obtain the magnetic field $\mathbf{H}_m$, where $\nabla_{\mathbf{r}}$ denotes the differentiation with respect to $\mathbf{r}$. Accuracy of this formula, however, becomes poor as the calculation point $\mathbf{r}$ approaches the boundary Γ because of the quasi singularity in $\nabla_{\mathbf{r}}G$ and $\nabla_{\mathbf{r}}\partial G/\partial n'$. To overcome this difficulty, introducing the correspondence

$$u \rightarrow \phi_2(\mathbf{r}') - \phi_2(\mathbf{r}_0) - \frac{\partial\phi_2(\mathbf{r}_0)}{\partial x_j}(x_j' - x_{0j}),$$

$$v \rightarrow \frac{\partial G(\mathbf{r}';\mathbf{r})}{\partial x_i}, \tag{13}$$

in (8), we get for $\mathbf{r}\in\Omega_2$

$$\frac{\partial\phi_2(\mathbf{r})}{\partial x_i} = -\int_\Gamma \left[\frac{\partial G(\mathbf{r}';\mathbf{r})}{\partial x_i}\left(\frac{\partial\phi_2(\mathbf{r}')}{\partial x_j'} - \frac{\partial\phi_2(\mathbf{r}_0)}{\partial x_j}\right) n_j' \right.$$
$$\left. - \frac{\partial^2 G(\mathbf{r}';\mathbf{r})}{\partial x_i\,\partial n'}\left\{\phi_2(\mathbf{r}') - \phi_2(\mathbf{r}_0) - \frac{\partial\phi_2(\mathbf{r}_0)}{\partial x_j}(x_j' - x_{0j})\right\} \right] d\Gamma', \tag{14}$$

where $i, j = 1, 2, 3$ and x_1, x_2, x_3 are the Cartesian coordinates, n_j the x_j-component of $\mathbf{n}$ and $\mathbf{r}_0$ is the reference point on Γ which is nearest to the calculation point $\mathbf{r}$. In (14), since the coefficients of the

Transactions on Modelling and Simulation vol 3, © 1993 WIT Press, www.witpress.com, ISSN 1743-355X

derivatives of G reduce those quasi singularity, the accuracy is expected to be effectively improved. This method is thought to be a natural extension of the regularized formula for potentials [2].

A similar but different regularization procedure can also be derived, that is, the introduction of the correspondence in (8)

$$u \to \phi_2(\mathbf{r}') - \phi_2(\mathbf{r}) - \frac{\partial \phi_2(\mathbf{r})}{\partial x_j}(x_j' - x_j),$$
$$v \to \frac{\partial G(\mathbf{r}'; \mathbf{r})}{\partial x_i}, \tag{15}$$

yields for $\mathbf{r} \in \Omega_2$

$$\frac{\partial \phi_2(\mathbf{r})}{\partial x_i} = -\int_\Gamma \left[\frac{\partial G(\mathbf{r}'; \mathbf{r})}{\partial x_i} \left\{ \frac{\partial \phi_2(\mathbf{r}')}{\partial n'} - \frac{\partial \phi_2(\mathbf{r})}{\partial x_j} n_j' \right\} - \frac{\partial^2 G(\mathbf{r}'; \mathbf{r})}{\partial x_i \partial n'} \left\{ \phi_2(\mathbf{r}') - \phi_2(\mathbf{r}) - \frac{\partial \phi_2(\mathbf{r})}{\partial x_j}(x_j' - x_j) \right\} \right] d\Gamma'. \tag{16}$$

One can see that the coefficients of the derivatives of G in (16) again reduce the quasi singularity. The value of $\phi_2(\mathbf{r})$ in (16) is determined through the regularization technique for potentials [3], *i.e.*,

$$\phi_2(\mathbf{r}) = -\int_\Gamma \left[G(\mathbf{r}'; \mathbf{r}) \frac{\partial \phi_2(\mathbf{r}')}{\partial n'} - \phi_2(\mathbf{r}') \frac{\partial G(\mathbf{r}'; \mathbf{r})}{\partial n'} \right] d\Gamma' \Big/ \left(1 + \int_\Gamma \frac{\partial G(\mathbf{r}'; \mathbf{r})}{\partial n'} d\Gamma' \right), \tag{17}$$

which is readily derived by considering the correspondence in (8).

$$u \to \phi_2(\mathbf{r}') - \phi_2(\mathbf{r}),$$
$$v \to G(\mathbf{r}'; \mathbf{r}). \tag{18}$$

The simultaneous equation (16) is then solved for $\partial \phi_2 / \partial x_i(\mathbf{r})$.

NUMERICAL RESULTS

The methods described in the previous section are now applied to an analysis of the two dimensional magnetic field outside the magnetic material of a rectangular cross section shown in Fig. 2. The external field is produced by the two straight coils with opposite current directions. The relative permeability μ of the magnetic material is taken to be 10.0. In the computations, the surface Γ is uniformly subdivided into 28 linear boundary elements.

Figures 3 and 4 show the resultant magnetic fields on the lines aa′ ($y = 4.2 \times 10^{-2}$) and bb′ ($x = 3.2 \times 10^{-2}$), respectively. In these figures,

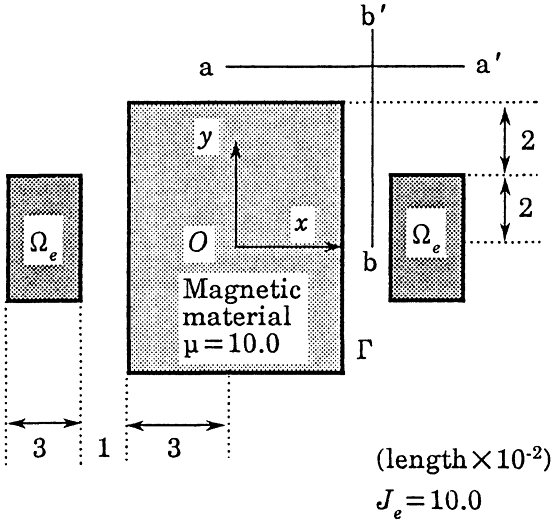

Fig. 2 A rectangular magnetic material with current region Ω_e. Computations of magnetic fields are performed on lines aa'($y=4.2\times10^{-2}$) and bb'($x=3.2\times10^{-2}$).

'Conventional', 'Method 1' and 'Method 2' denote the results calculated by (12), (14) and (16), respectively. The values of $\partial\phi_2(r_0)/\partial x_j$ in (14) are determined from the flux $\partial\phi/\partial n$ and the finite difference of ϕ on Γ. The number (n) in the figures represents the number of points for the Gaussian quadrature.

From Figs. 3 and 4, one can see that the results by the present methods, in which the four points Gaussian quadrature is employed, agree well with those by 'Conventional (12)'. In contrast to this, 'Conventional (4)' obviously gives the unphysical results as shown in Fig. 3 (b) and Fig. 4.

Figure 5 shows the magnetic field distribution near the upper right corner of the magnetic material. Apparently, the conventional method gives inaccurate field vectors near the boundary, whereas the present methods provide reasonable solutions. The extraordinary approach of the computational points to the boundary seems to give rise to slight errors in Method 2, which are however negligible compared to those by the conventional method.

Transactions on Modelling and Simulation vol 3, © 1993 WIT Press, www.witpress.com, ISSN 1743-355X

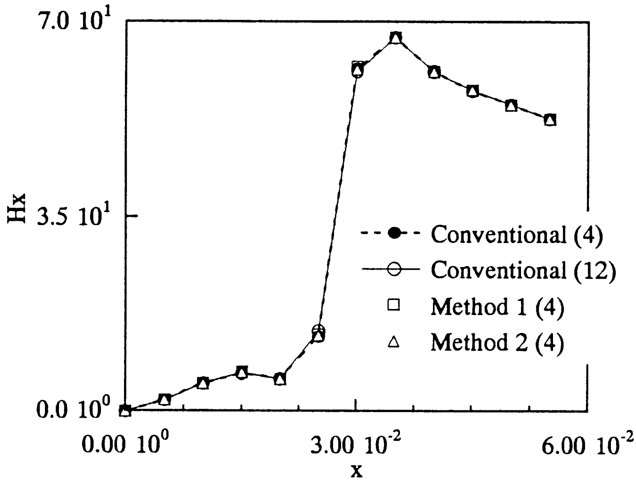

(a) H_x component

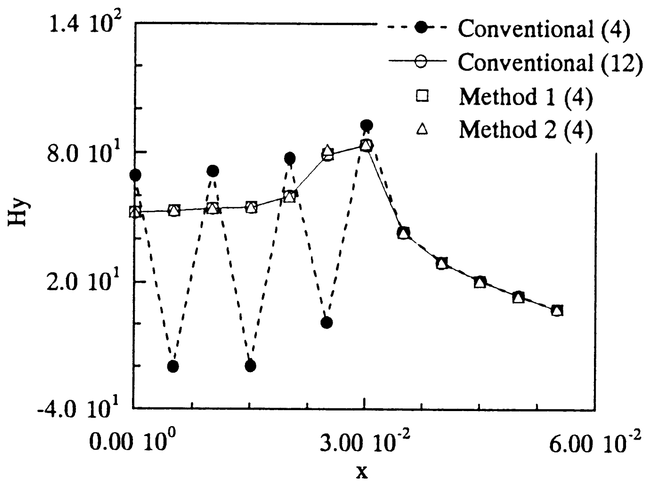

(b) H_y component

Fig. 3 Profiles of magnetic field H on the line aa′. The number (n) denotes the number of points for the Gaussian quadrature. 'Conventional', 'Method 1' and 'Method 2' denote the results calculated by (12), (14) and (16), respectively.

Transactions on Modelling and Simulation vol 3, © 1993 WIT Press, www.witpress.com, ISSN 1743-355X

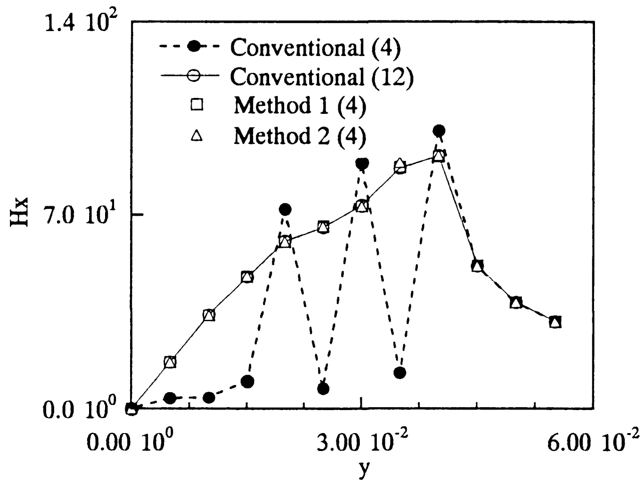

(a) H_x component

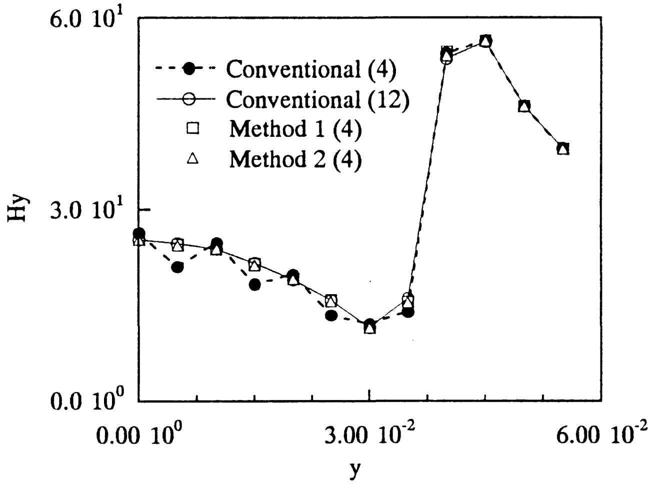

(b) H_y component

Fig. 4 Profiles of magnetic field H on the line bb'.

Transactions on Modelling and Simulation vol 3, © 1993 WIT Press, www.witpress.com, ISSN 1743-355X

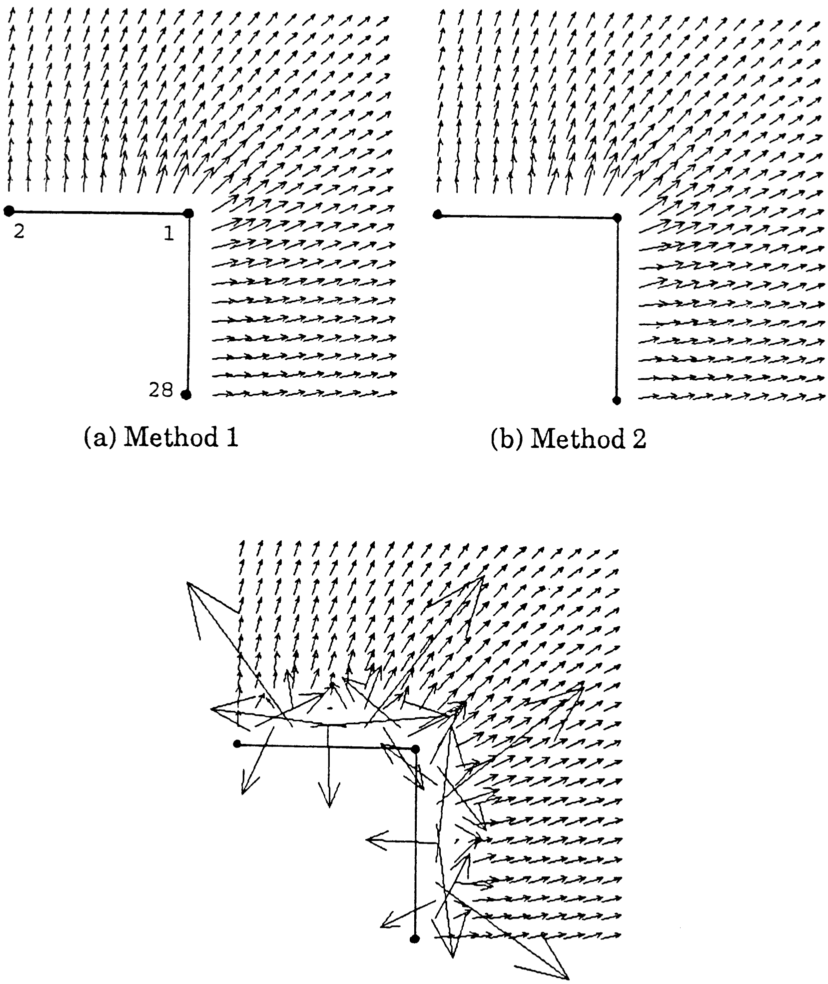

Fig. 5 Magnetic field distributions near the upper right corner of the magnetic material shown in Fig. 2. The dots represent the nodal points and their numbers are indicated in (a). The four points Gaussian quadrature is employed in all computations.

The computer implementation of Method 1 involves a finding procedure of the reference points and computation of the potentials and fluxes on them while that for Method 2 needs few additional calculations of the coefficients in (16). From our experience, the present methods neither need much effort for computer implementation overall nor consume computer time.

SUMMARY

This paper has described the computational methods for magnetic fields, which effectively regularize the quasi singularity in the kernel. It has been shown that the present methods do not suffer from deterioration of accuracy in the computation of magnetic field near surfaces.

REFERENCES

[1] Igarashi, H. and Honma, T., 'Accurate Boundary Element Method for Potential Fields Near Boundaries,' submitted.
[2] Kisu, H. and Kawahara T., 'Boundary Element Analysis System Based on a Formulation with Relative Quantity,' *Boundary Elements X*, (ed. C.A. Brebbia), Vol.1, pp. 111-121, Springer-Verlag, Berlin, 1988.
[3] Enokizono M. and Todaka T., 'Boundary Element Analysis Using Revised Integration,' (in Japanese) *Trans. IEE Japan*, Vol. 106-A, pp. 149-156, 1986.